Notch filters in soliton communications systems: a comparison

Andrew Docherty and Pak L. Chu

Optical Communications Group, School of Electrical Engineering, University of New South Wales, Sydney 2052, Australia

Boris A. Malomed

Department of Interdisciplinary Studies, Faculty of Engineering, Tel Aviv University, Tel Aviv 69978, Israel

Received February 23, 2001; revised manuscript received September 10, 2001

A detailed analysis of the dynamics of classical (sech) and dispersion-managed solitons is developed for a channel guided by filters of different types, with emphasis on comparison of results produced by etalon and notch filters. By means of analytical approximations, based on balance equations for the soliton's energy and momentum, we demonstrate that finite-width notch filters can be as efficient as etalon filters, and attainable filter efficiency is higher for dispersion-managed solitons than for classical solitons. We also show that values for filter parameters can be found that maximize the filter's restoring force. © 2002 Optical Society of America

OCIS codes: 060.2310, 060.4510, 060.5530, 060.2340, 190.5530, 190.4370.

1. INTRODUCTION

Fundamental limiting factors for high-bit-rate optical communications are interchannel timing jitter caused by collisions between solitons in different channels in a wavelength-division-multiplexed (WDM) system, four-wave mixing, intra-channel Gordon–Haus timing jitter, and intrachannel interactions of pulses in adjacent bit periods. The effect of these factors can be assuaged by the introduction of dispersion management[1–5] and by filters.[2]

Filters have been shown to produce beneficial effects on the suppression of interactions between solitons[6–8] and the Gordon–Haus jitter inside one channel.[9–12] Generally, filters help to stabilize the solitons' energies and widths,[13] which is also the case for dispersion management,[14,15] although the effect is weaker.[16] A dispersion-management system with filters can also be subject to instabilities.[17]

In a dense WDM system, soliton channels should be spaced closely to maximize the spectral efficiency, which in practice implies a wavelength separation between the channels of $\delta\lambda < 1$ nm. As the channels are pushed closer, the traditional bandpass filters are no longer relevant, and whatever types of filter are used in such a system, they are effectively notch filters (NFs). It is therefore important to analyze how NFs affect the propagation of solitons and their effectiveness at suppressing the jitter. In this context, NFs were recently considered in Refs. 18 and 19, where they were approximated, in the spectral domain, by delta functions bounding the soliton-carrying channel. However, infinitely narrow notches are not feasible in practice, nor do they give the best results. This makes it necessary to study soliton transmission with realistic finite-width NFs, which is the main subject of the present paper.

NFs can be fabricated on the basis of chirped fiber Bragg gratings.[20,21] Another physical idea, to use quantum dots the size of ~100 nm, has been proposed.[18] Equidistant spectral notches are induced through resonant absorption of photons by electrons trapped in the dot.

The suppression of cross talk (i.e., the effects produced by collisions between solitons in adjacent channels of a WDM system) by NFs has already been considered in some detail.[18,19] In this paper we focus on the stabilization effects inside a single channel bounded by a pair of NFs. It is especially interesting to compare the stabilization of a channel by NFs in comparison with the usual etalon filters.

We analyze NFs with square notches and also with Gaussian notches. General equations valid for any filter shape are derived in the process. We present results for the propagation of classical (ordinary) and dispersion-managed (DM) solitons in a system with square and Gaussian NFs, using both perturbation theory and direct numerical simulations.

A method for comparing efficiencies of different filters is developed in the following way: As the filters cause additional energy loss, one needs to increase accordingly the gain provided by the amplifiers, which are inserted into the fiber link to compensate for the background fiber and filter losses and are usually packaged together with the filters. The most practical approach to compare different filters is to compare the magnitude of the filters' restoring force against the amount of excess gain needed, enabling a comparison to be made between filters of various types and widely differing parameters. The filter's restoring force is effectively the filters ability to suppress fluctuations of the central frequency of the soliton from the center of the channel. This technique enables a com-

0740-3224/2002/020190-08$15.00

parison to be made between NFs and standard bandpass filters, in terms of guiding a soliton in one channel. Our general result is that, for a single channel, the etalon and notch filters are equally efficient; however, it should be borne in mind that filters with a true parabolic profile are irrelevant for dense WDM systems.

The rest of the paper is organized as follows. In Section 2 we develop an analytical approach to the study of the dynamics of classical and DM solitons with filters of an arbitrary spectral shape, based on the balance equations for the soliton's energy and momentum. Section 3 is devoted to a comparison of the efficiency of different types of filters. The comparison is made both with an analytical perturbation approach and by means of direct numerical simulations, the analytical and numerical results being in good agreement. Whereas in the main part of the paper we consider only models with filtering that is uniformly distributed along the fiber link, Section 4 concerns the results of simulations of a more realistic *lumped* model with discrete filters, concluding that the discreteness produces a nearly negligible effect on final results.

2. PERTURBATION ANALYSIS OF GENERAL FILTERING

The standard nonlinear Schrödinger equation (NLSE) governing the evolution of the slowly varying amplitude $u(z, \tau)$ in the fiber can be transformed to a dimensionless form, measuring the propagation length and time in units of the dispersion length $z_* = 2\pi c t_*^2/\lambda^2 \bar{D}$ and characteristic time $t_* = \tau/c_\tau$, where c and λ are the velocity and wavelength of the electromagnetic wave, τ is the FWHM width of a basic pulse to be considered, c_τ is a constant dependent on the type of pulse being considered, and $\bar{D}$ is the average dispersion value. This yields the NLSE, which includes a filtering operator f, which we here take in the distributed approximation, filtering strength ϵ, excess gain α_0 that compensates solely for the energy lost due to the filter, a dimensionless dispersion coefficient $D(z)$, which is variable in the case of DM, or $D \equiv 1$ in the case of classical solitons:

$$i\frac{\partial u}{\partial z} + \frac{D(z)}{2}u_{tt} + |u|^2 u = i\epsilon f(u,t) + i\alpha_0 u,$$

assuming that there is no fiber loss or, equivalently, that the filter acts over a distance significantly longer than the amplifier spacing.

For the analysis of filters acting in the frequency domain, it is natural to rewrite the NLSE in the Fourier domain as defined by $\hat{u}(z,\omega) \equiv (1/\sqrt{2\pi})\int_{-\infty}^{\infty} \exp(i\omega t) \times u(z,t)\mathrm{d}t$, giving

$$i\frac{\partial \hat{u}}{\partial z} - \frac{D(z)}{2}\omega^2 \hat{u} + i\int_{-\infty}^{\infty} |u|^2 u \exp(i\omega t)\mathrm{d}t = i\epsilon F(\omega)\hat{y} + i\alpha_0 \hat{u}, \quad (1)$$

where the transmission function $F(\omega)$ represents the filtering operator in the frequency domain, which can be derived from the filter transfer function for the distributed and lumped filter models.[22] For the standard etalon filter centered at a frequency ω_* the transmission function is parabolic: $F_e(\omega) = -(\omega - \omega_*)^2$. From Eq. (1) it is straightforward to derive evolution equations for the energy

$$E \equiv \int_{-\infty}^{\infty} |\hat{u}(\omega)|^2 \mathrm{d}\omega = \int_{-\infty}^{\infty} |u(t)|^2 \mathrm{d}t$$

and momentum

$$M \equiv \int_{-\infty}^{\infty} \omega |\hat{u}(\omega)|^2 \mathrm{d}\omega = i\pi \int_{-\infty}^{\infty} (u^* u_t - u u_t^*)\mathrm{d}t$$

of the soliton, assuming the filter strength ϵ is sufficiently small so as not to overly perturb the assumed soliton shape. These balance equations can then be used to describe the evolution of a soliton in the quasi-particle approximation.[18,19] The balance equations are

$$\frac{\partial}{\partial z}\int_{-\infty}^{\infty} |\hat{u}|^2 \mathrm{d}\omega = 2\epsilon \int_{-\infty}^{\infty} \Re[F(\omega)]|\hat{u}|^2 \mathrm{d}\omega + 2\alpha_0 \int_{-\infty}^{\infty} |\hat{u}|^2 \mathrm{d}\omega, \quad (2)$$

$$\frac{\partial}{\partial z}\int_{-\infty}^{\infty} \omega|\hat{u}|^2 \mathrm{d}\omega = 2\epsilon \int_{-\infty}^{\infty} \omega\Re[F(\omega)]|\hat{u}|^2 \mathrm{d}\omega + 2\alpha_0 \int_{-\infty}^{\infty} \omega|\hat{u}|^2 \mathrm{d}\omega. \quad (3)$$

It is noted that these equations are dependent only on the real part, $\Re[F(\omega)] \equiv F_r(\omega)$, of the filter function, its imaginary part being a contribution only to the dispersion. Equation (2) determines the excess gain required for the energy equilibrium, $\mathrm{d}E/\mathrm{d}z = 0$, which gives an equation for α_0 in terms of a steady-state soliton solution, $\hat{u}(\omega, z) = \hat{u}_0(\omega)$:

$$\alpha_0 = -\epsilon \frac{\int_{-\infty}^{\infty} F_r(\omega)|\hat{u}_0(\omega)|^2 \mathrm{d}\omega}{\int_{-\infty}^{\infty} |\hat{u}_0|^2 \mathrm{d}\omega}. \quad (4)$$

To proceed with the analysis, it is necessary to specify the filter profile and pulse shape. In this vein, first classical solitons are investigated, and then DM solitons.

A. Classical Soliton Case

The Fourier transform of the classical (non-DM) soliton with time-domain amplitude (and inverse width) η and central frequency Ω is

$$\hat{u}(z,\omega) = \pi \operatorname{sech}\frac{\pi}{2\eta(z)}[\omega - \Omega(z)],$$

assuming that the (constant) dispersion and nonlinearity coefficients are $D = g = 1$. Substituting this into Eqs. (2) and (3), we arrive at a dynamical system for the amplitude and central frequency of the classical soliton,

$$\frac{\partial \eta}{\partial z} = 2\alpha\eta(z) + \frac{\pi}{2}\epsilon\int_{-\infty}^{\infty} F_r(\omega) \times \operatorname{sech}^2\frac{\pi}{2\eta(z)}[\omega - \Omega(z)]\mathrm{d}\omega, \quad (5)$$

$$\frac{\partial \Omega}{\partial z} = \frac{\pi}{2\eta}\epsilon\int_{-\infty}^{\infty}[\omega - \Omega(z)]F_r(\omega) \times \operatorname{sech}^2\frac{\pi}{2\eta(z)}[\omega - \Omega(z)]\mathrm{d}\omega. \quad (6)$$

From this system we can find the excess gain required for the existence of an equilibrium state with a constant amplitude η_0, as

$$\alpha_0 = -\frac{\pi}{4\eta_0}\epsilon\int_{-\infty}^{\infty} F_r(\omega)\operatorname{sech}^2\frac{\pi}{2\eta_0}(\omega - \Omega_0)\mathrm{d}\omega, \quad (7)$$

where the equilibrium value Ω_0 of the central frequency must coincide with the center of the bandpass of $F(\omega)$.

B. Dispersion-Managed Soliton Case

For DM solitons it is more difficult to obtain a concise analytic representation for the Fourier representation of the pulse shape $\hat{u}_{\mathrm{DM}}(\omega, z)$. Usually, it is close to a Gaussian (which is an exact solution to the original NLSE in the linear limit)[23]:

$$|\hat{u}_{\mathrm{Gauss}}(\omega, z)|^2 = a(z)^2\exp\{-b(z)[\omega - \Omega(z)^2]\}, \quad (8)$$

with an energy given by $E_{\mathrm{Gauss}} = a^2\sqrt{\pi/b}$. The amplitude and inverse width, $a(z)$ and $b(z)$, can be determined by matching this expression to the real DM soliton, $\hat{u}_{\mathrm{DM}}(\omega, z)$, obtained by means of various asymptotic approaches[23–26] or through numerical averaging.[27] In particular, a and b can be related by the following model equation[25]:

$$a^2 = \sqrt{2}\bar{D}\frac{S}{b}\frac{1 + (S/b)^2}{\sinh^{-1}(S/b)}, \quad (9)$$

(recall that $\bar{D}$ is the average dispersion), where S is the usual DM map strength.[27]

The validity of the Gaussian approximation is justified by results presented in Fig. 1, which shows the relative difference in the energy between a numerically found DM mode $\hat{u}_{\mathrm{DM}}(\omega)$ and the Gaussian approximation Eq. (8) with the parameters a, b, and Ω obtained by minimization of the L^2 difference norm,

$$N \equiv \int_{-\infty}^{\infty}[|u_{\mathrm{DM}}(\omega)| - a\exp(-b\omega^2/2)]^2\mathrm{d}\omega. \quad (10)$$

Figure 1 suggests that, for moderate energies, the Gaussian approximation may be expected to give answers accurate to a few percent.

Substituting the approximation Eq. (8) into Eqs. (2) and (3), we derive the evolutional equations for E and Ω:

$$\frac{\mathrm{d}E}{\mathrm{d}z} = 2\alpha_0 E + 2\epsilon\int_{-\infty}^{\infty} F_r(\omega)a(z)^2 \times \exp\{-b(z)[\omega - \Omega(z)]^2\}\mathrm{d}\omega, \quad (11)$$

$$\frac{\mathrm{d}\Omega}{\mathrm{d}z} = \frac{2}{E(z)}\epsilon\int_{-\infty}^{\infty}[\omega - \Omega(z)]F_r(\omega)a(z)^2 \times \exp\{-b(z)[\omega - \Omega(z)]^2\}\mathrm{d}\omega. \quad (12)$$

As in the case of Eq. (4), the excess gain required for an equilibrium state with constant values of the amplitude a_0 and inverse width b_0 of the Gaussian pulse is

$$\alpha_0 = -\epsilon\sqrt{\frac{b_0}{\pi}}\int_{-\infty}^{\infty} F_r(\omega)\exp[-b_0(\omega - \Omega_0)^2]\mathrm{d}\omega, \quad (13)$$

where Ω_0 again coincides with the center of the profile $F(\omega)$. Note that α_0 does not depend on the soliton's amplitude a_0.

As opposed to the classical soliton, where Eqs. (5) and (6) provided a closed dynamical system, the system for the DM soliton is not closed, as there are only two equations for the three variables a, b, and Ω. To complete the system, we can use the relation between a and b from Eq. (9). Making use of Eq. (11), we obtain[16]

$$\frac{\mathrm{d}a}{\mathrm{d}z} = 2a\frac{\alpha + \epsilon\sqrt{\frac{b}{\pi}}\int_{-\infty}^{\infty} F_r(\omega)\exp[-b(\omega - \Omega)^2]\mathrm{d}\omega}{2 - (a/2b)\mathrm{d}b/\mathrm{d}a},$$

$$\frac{\mathrm{d}b}{\mathrm{d}z} = 2a\frac{\alpha + \epsilon\sqrt{\frac{b}{\pi}}\int_{-\infty}^{\infty} F_r(\omega)\exp[-b(\omega - \Omega)^2]\mathrm{d}\omega}{2\mathrm{d}a/\mathrm{d}b - a/2b}. \quad (14)$$

This system can be solved numerically. In Fig. 2, the result is compared with that obtained from direct simulations of the underlying NLSE, where a and b are found from the minimization of the norm (10) of $\hat{u}_{\mathrm{DM}}$ sampled at points along z. We also compare the results to an intermediate approximation, where the energy-evolution Eq. (11) is solved numerically, by use of $a(E)$ and $b(E)$ as obtained from numerically found stationary DM solitons in the model without filters or excess gain.

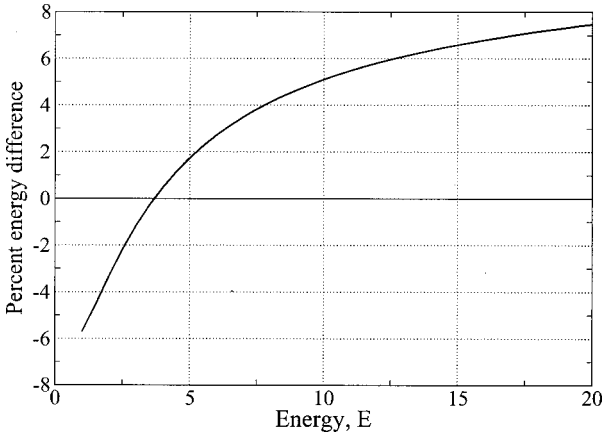

Fig. 1. Relative energy difference between a numerically exact dispersion-managed soliton (with a map strength $S = 2$) and the best-fit Gaussian approximation to it, versus the net energy of the numerically found soliton.

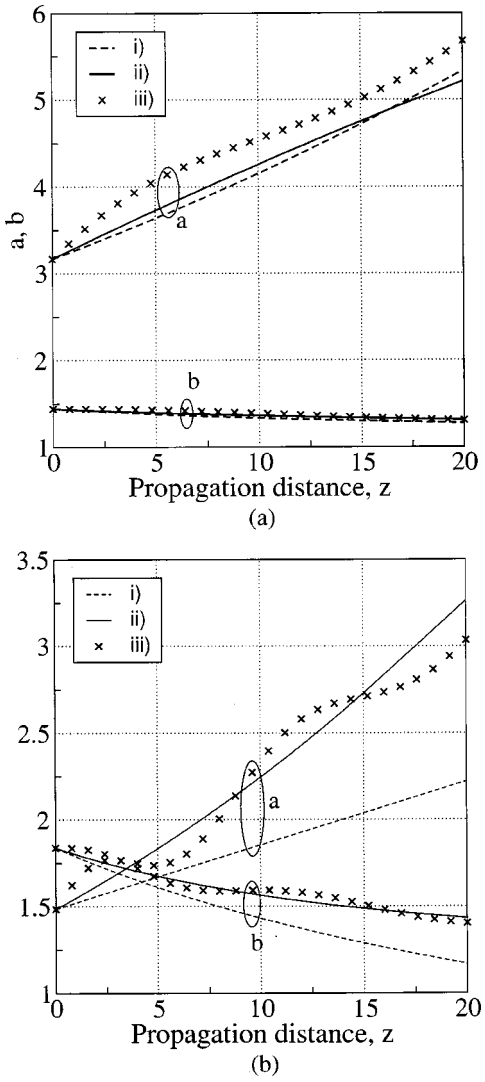

Fig. 2. Comparison between amplitude a and inverse width b of the Gaussian pulse of Eq. (8) with etalon filterering ($\epsilon = 0.1$), (i) from numerical solution of the analytically derived Eqs. (14), (ii) from numerical solution of the energy-evolution Eq. (11) with $a(E)$ and $b(E)$ taken from numerically generated stationary DM solitons, and (iii) from direct numerical simulations of the NLSE (1).

Figure 2 shows that, although both approximations give good results at low energies of the soliton, the one that uses $a(E)$ and $b(E)$ as found from the numerically exact stationary DM solitons is considerably more accurate at higher energies.

C. Notch Filters

For the standard etalon filters (recall that the strength of the filtering is controlled by the separate parameter ϵ), the perturbation method outlined above reproduces the same results that were obtained for the classical solitons[28] and for DM solitons.[14,16] New filter models that are examined here are NFs with the following square and Gaussian profiles:

$$F_S = \begin{cases} 1 & \text{if } |\omega - \omega_0^{(1,2)}| < \nu_s/2 \\ 0 & \text{otherwise} \end{cases}, \tag{15}$$

$$F_G = \sum_{m=1,2} \exp\left[-\frac{1}{\nu_g}(\omega - \omega_0^{(m)})^2 \right], \tag{16}$$

i.e., two notches that define a soliton-transmission channel between them (a "soliton rail"). Here $\omega_0^{(1,2)}$ are the locations of the notches' centers, and ν_s and ν_g determine the width of the square and the Gaussian notches, respectively.

To analyze the effects of the filters, we insert Eq. (15) or (16) into the evolution equations for energy and momentum, i.e., Eqs. (5) and (6) for classical solitons or Eqs. (11) and (12) for DM ones. In particular, the resulting evolution equations for the classical soliton take a simple form in the case when the Gaussian notches are narrow in comparison with the soliton in the frequency domain ($\nu_g \to 0$):

$$\left(\frac{dE}{dz}\right)_{\text{sech}} \simeq 4\alpha_0\eta - \epsilon\pi^{3/2}\sqrt{\nu_g}\left[\text{sech}^2\frac{\pi}{2\eta}(\omega_0 - \Omega) + \text{sech}^2\frac{\pi}{2\eta}(\omega_0 + \Omega) \right],$$

$$\left(\frac{d\Omega}{dz}\right)_{\text{sech}} \simeq \epsilon\frac{\pi^{3/2}\sqrt{\nu_g}}{2\eta}\left[(\Omega - \omega_0)\text{sech}^2\frac{\pi}{2\eta}(\omega_0 - \Omega) + (\Omega + \omega_0)\text{sech}^2\frac{\pi}{2\eta}(\omega_0 + \Omega) \right]. \tag{17}$$

For DM solitons we can also arrive at a simplification for narrow Gaussian notches:

$$\left(\frac{dE}{dz}\right)_{\text{DM}} \simeq 2\alpha_0 E - 2\epsilon\sqrt{\pi\nu_g}a^2\{\exp[-b(\omega_0 - \Omega)^2] + \exp[-b(\omega_0 + \Omega)^2]\},$$

$$\left(\frac{d\Omega}{dz}\right)_{\text{DM}} \simeq -\frac{2\epsilon}{E}a^2\sqrt{\pi\nu_g}\{(\omega_0 - \Omega)\exp[-b(\omega_0 - \Omega)^2] + (\omega_0 + \Omega)\exp[-b(\omega_0 + \Omega)^2]\}. \tag{18}$$

The results for square filters are in fact identical, with the correspondence $\nu_g = \nu_s^2/\pi$. Realizing a Gaussian of the form $a[\exp(-x^2/\nu)]$ with amplitude a and width ν in the limit of $\nu \to \infty$ and $a \to \sqrt{\nu/\pi}$ becomes equivalent to the Dirac delta function. With this relation these equations coincide with those that have been derived in the simplest model with infinitely narrow (δ-like) notches.[18,19] A real difference appears if one considers the realistic case of finite-width notches, as is shown below.

3. FILTER COMPARISONS

In the previous section we derive equations for the evolution of energy and momentum of classical and DM solitons in one channel guided by filters of various types. To decide upon the relative merits of different types of filters, we must first define what a filter's efficiency is.

Linearizing the equation for $d\Omega/dz$ about Ω_0, the equilibrium point, we have

$$\frac{d\Omega}{dz} = -H(\Omega - \Omega_0) + O[(\Omega - \Omega_0)^2], \tag{19}$$

where we assert that H is a measure of the "restoring force" induced by a filter. For the etalon filter a well-known result of perturbation theory is $H = (4/3)\epsilon\eta^2$, if the filter acts upon classical solitons, and $H = 2\epsilon/b$ for DM solitons, where the same notation as in Section 2 is used.[14,15]

Considering a general filter type, we linearize Eq. (6) for classical solitons, which yields (assuming without loss of generality that $\Omega_0 = \omega_* = 0$)

$$H = -\frac{\pi}{2\eta}\epsilon\int_{-\infty}^{\infty} F_r(\omega)\mathrm{sech}^2\frac{\pi\omega}{2\eta}\left(\frac{\pi\omega}{\eta}\tanh\frac{\pi\omega}{2\eta} - 1\right)d\omega. \tag{20}$$

For DM solitons we similarly find from Eq. (12)

$$H = -2\epsilon\sqrt{\frac{b}{\pi}}\int_{-\infty}^{\infty} F_r(\omega)(2\omega^2 b - 1)\exp(-b\omega^2)d\omega. \tag{21}$$

The effectiveness of guiding filters can be measured by the magnitude of H, as it determines the strength of the suppression of perturbations in the propagation of the solitons. However, one simultaneously has to take into regard the size of the excess gain needed by the filters to ensure stable propagation. Thus we require the strongest "restoring force" with the lowest excess gain. This implies that a meaningful comparison can only be made by taking the same excess gain for each different filter type.

In the case of etalon filters, the above analytical considerations amount to the simple result $H = 4\alpha_0$ for both classical and DM solitons, i.e., the filter effectiveness depends solely on the excess gain. Filters of an arbitrary type may be compared by first fixing the excess gain through the Eqs. (7) and (13) (which were derived from the energy-balance condition) for classical and DM solitons, respectively. If other parameters are available, their values should be chosen to maximize the value of H. This gives a definite value of H itself, and the most effective filters are those that give the highest value of H.

The etalon filters have only one parameter, ϵ. For given α_0, the above energy-balance condition yields

$$\epsilon_{\mathrm{sech}} = 3\alpha_0/\eta, \quad \epsilon_{\mathrm{DM}} = 2b\alpha_0, \tag{22}$$

for classical and DM solitons, respectively. The finite-width NFs introduced above have three parameters: ϵ, ν, and ω_0. In the process of the optimization of $H(\epsilon, \nu, \omega_0)$, constrained by the balance equation (7) or Eq. (13) for the excess gain, two parameters are fixed, leaving one free coefficient that may be varied arbitrarily. Assuming the perturbation assumptions remain valid, any filter's effectiveness can theoretically be matched by this free variable.

A. Results of Filter Comparisons with the Analytical Approximation

The simplest analytical approximation based on Eqs. (17) and (18) is not appropriate for the optimization procedure, as an essential result for NFs is that wide notches are far more effective than narrow ones, whereas these approximate equations pertain to narrow notches. The general analytically derived Eqs. (5), (6) and Eqs. (11), (12) can be used for any arbitrary filter shape, provided the integrals can be calculated numerically.

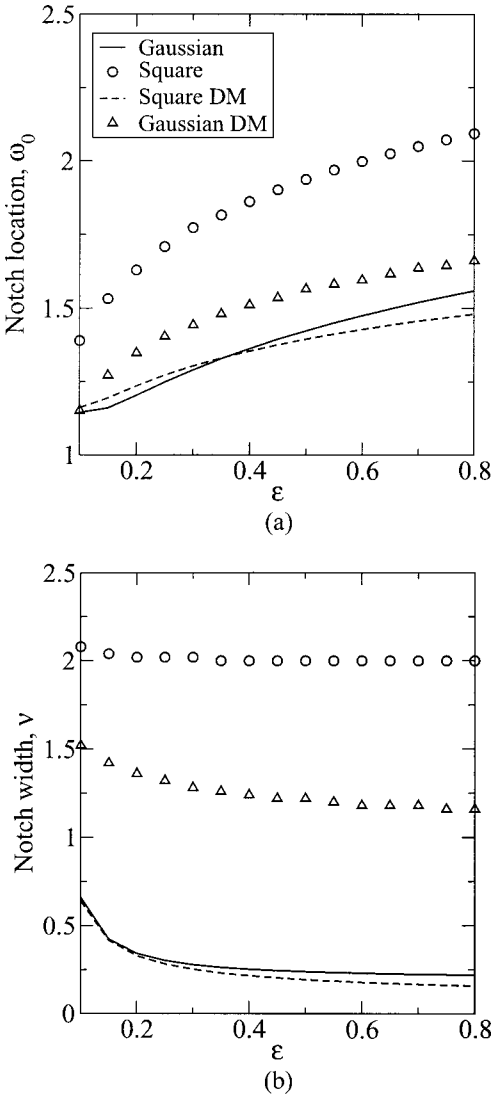

Fig. 3. Optimal values of ν (a) and ω_0 (b) versus ϵ for classical and DM solitons, with $\alpha_0 = 0.05$ for Gaussian and square-notch filters, as obtained from Eqs. (5), (6) and Eqs. (11), (12) with integrals calculated numerically.

Starting with classical solitons, we choose the excess gain to be $\alpha_0 = 0.05$ and set $\eta = 1$, so that Eq. (22) yields the equilibrium value $\epsilon_e = 0.15$ for the etalon filters acting upon the classical solitons. A DM pulse is taken with $b = 1.5$, so that Eq. (22) gives $\epsilon_e^{(\mathrm{DM})} = 0.15$ as well, and a meaningful comparison can be made.

The optimal values of ν and ω_0 are shown, as functions of ϵ, in Fig. 3. Using these plots, one can find values ϵ_s and ϵ_g of the strength ϵ for the square and Gaussian NFs that give the same value of H as that generated by the etalon (parabolic) filter, being 0.2 in the present case. This gives $\epsilon_g = 0.4327$, $\epsilon_s = 0.2589$, $\epsilon_g^{(\mathrm{DM})} = 0.3127$, $\epsilon_s^{(\mathrm{DM})} = 0.2184$. These values correspond to *matched* filters, those that, according to first-order perturbation theory, should behave identically.

B. Numerical Results

In this subsection we present results obtained for classical and DM solitons by *direct* simulations of the corresponding version of the NLSE, performed by means of the split-step method. We use a numerically exact initial DM mode calculated by numerical averaging,[27] with a pulse energy $E = 5$ corresponding to a width of $b = 1.5$. The Gaussian approximation of Eq. (8) used in the previous subsection was determined from this DM pulse by minimization of the L2 difference norm in Eq. (10). The DM map was taken in the form of two segments of equal lengths 0.05 with the values of the dispersion coefficient $D_1 = 79$ and $D_2 = -81$, which correspond to a DM map strength $S = 2$ and the average dispersion $\bar{D} = 1$.[27] In physical units, this is equivalent to $z = 4\,000$ km, with $\bar{D} = 0.2$ ps/(nm km) and the soliton's dispersion length $z_* = 200$ km and temporal width $t_* = 7.14$ ps.

Numerically we can test the relative effectiveness of filters by several criteria. The recentralization characteristic shows how quickly the filter brings a soliton initially spectrally offset by a small amount back to the filter's center. This gives us a good idea of the effectiveness of the filter in combatting the frequency jitter caused by incomplete soliton collisions between channels, which occur at the start of the transmission line when the solitons are initially overlapped. Note that Eq. (19) predicts exponential relaxation for a small initial offset. For the numerical tests, simulations with the initial soliton offset $\Omega(0) = 0.1$ were performed over the distance $z = 20$. An effective value of the restoration-force coefficient H [see Eq. (19)] can thus be obtained by matching the relaxation of the central frequency of the soliton to an exponential of the form $\Omega(z) = \Omega(0)\exp(-Hz)$.

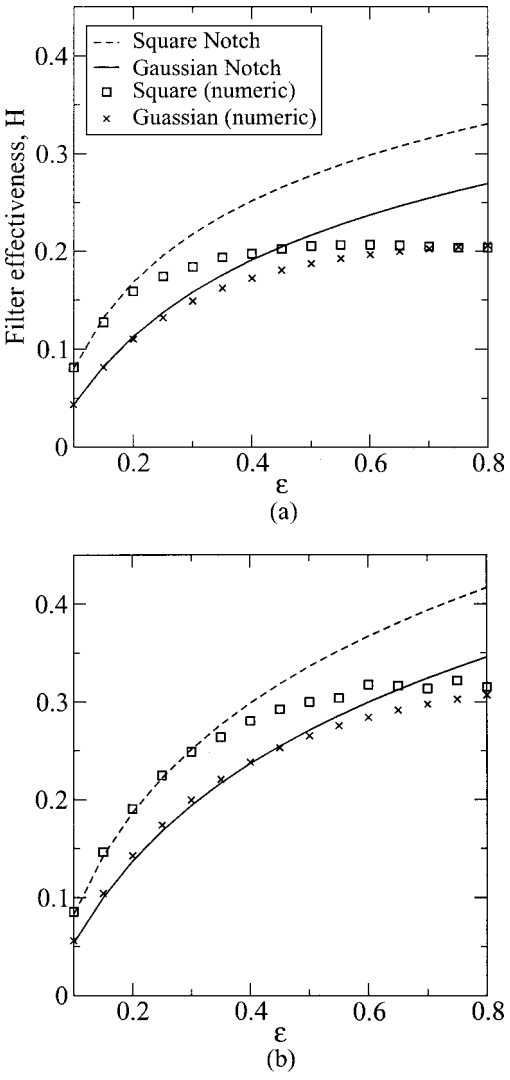

Fig. 4. Value of H versus ϵ for (a) classical solitons and (b) DM solitons as obtained from Eqs. (20) and (21) and from direct numerical simulations with $\alpha_0 = 0.05$.

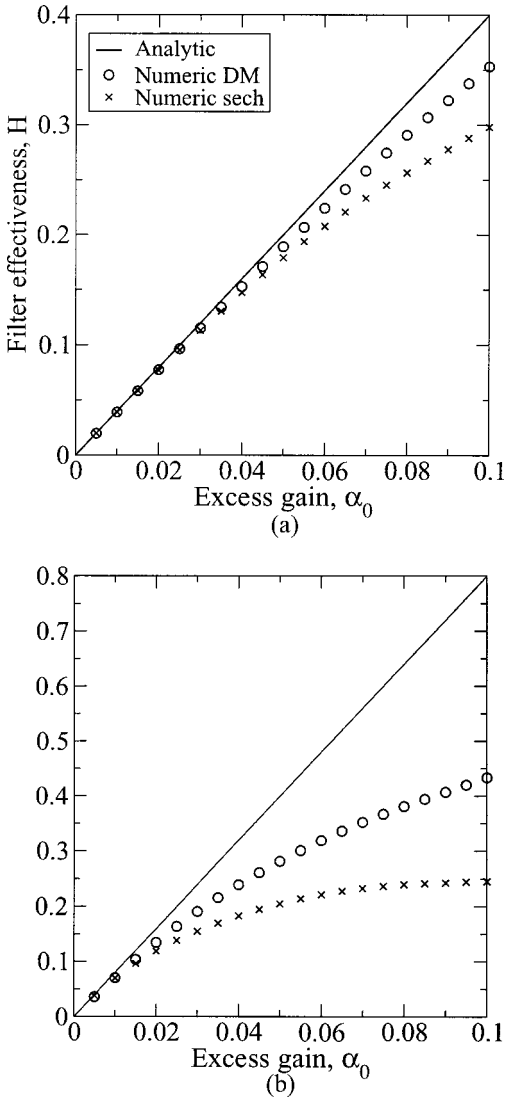

Fig. 5. Value of H versus α_0 for (a) the etalon and (b) Butterworth filters both numerically and analytically.

Figure 4 displays the analytical and numerical results for the filter effectiveness, H, as obtained with the square and Gaussian notches for both classical and DM solitons. It can be seen that a good agreement is obtained up to $\epsilon = 0.3$ and 0.4 for the square and Gaussian notches for the classical solitons, and $\epsilon = 0.4$ and 0.6 for the square and Gaussian notches for the DM solitons.

It is expected that as ϵ ceases to be small, the perturbation method will break down, and we can see this espe-

cially in the case of the square filters. The results for the Gaussian filters, however, remain close to the perturbative approximation for quite high values of ϵ, implying they are less liable to disturb the soliton from its assumed form at higher filter strengths.

The filter effectiveness, H, plateaus, with both square and Gaussian NFs, at $H \simeq 0.2$ for classical solitons irrespective of the increase in ϵ, which is the same value of H as attained with etalon (parabolic) filters for classical solitons. For DM solitons the filter effectiveness plateaus at $H \simeq 0.31$, which is *larger* than the $H = 0.2$ attained with the etalon filter for DM solitons. It thus appears that NFs are no more beneficial than the parabolic ones for systems using classical solitons, but notches can offer greater effectiveness for DM solitons. It also suggests that DM solitons are able to support stronger filters.

In this connection, it should be noticed that the analytical prediction for Butterworth filters analytically gives $H = 8\alpha_0 = 0.4$ for both classical and DM solitons[11]; however, looking at Fig. 5(b), we can see that this is not true at even moderate values of excess gain. Specifically at $\alpha_0 = 0.05$ (the same value that has been used with the previous notch filters) we get $H = 0.21$ for classical solitons and $H = 0.28$ for DM solitons, which are significantly lower than the analytic value. The results for the etalon filter are shown in Fig. 5(a), where it is seen that the analytic results are a good match to numerics. It appears that strong Butterworth filters do not give as good a performance as indicated by analytics and give filter effectiveness similar to notch filters. Also, the numerical results are significantly closer to analytics for DM solitons than for classical solitons; it seems that DM solitons allow for higher filter strengths.

It is not obvious that the size of the coefficient H necessarily translates into effectiveness of resistance to the timing jitter caused by random-frequency fluctuations, which simulate the behavior of a soliton subjected to interchannel soliton collisions.[12] To simulate this, the filters were tested in a run where an initially unperturbed soliton was subjected to random *lumped* perturbations of its central frequency. This was repeated ten times, and the corresponding rms values were computed. The same pseudo-random perturbations were applied to models equipped with different filters. The results are shown in Fig. 6. It can be seen that there is a distinct reduction in the filtered timing jitter as opposed to the unfiltered and that the reductions provided by all three different types of filters are very similar.

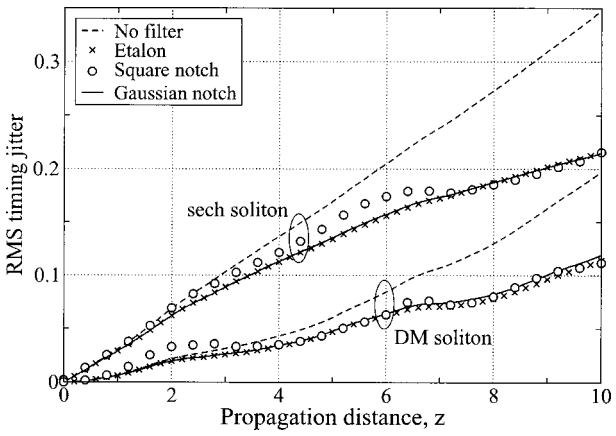

Fig. 6. Direct test of frequency-jitter suppression. The plots show the temporal offset for (a) classical solitons and (b) DM solitons versus the propagation distance. Note that although the filter effectiveness is the same for both classical and DM solitons ($H = 4\alpha_0$), the frequency jitter translates to timing jitter differently for both, the DM solitons having significantly less consequent timing jitter.

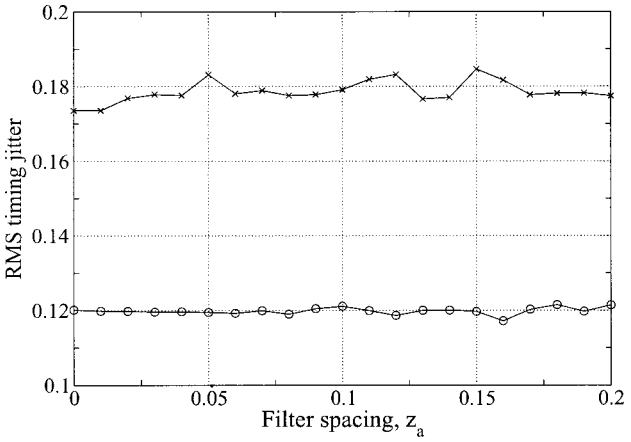

Fig. 7. Final values of the timing jitter in the lumped version of the dispersion-managed model with the Gaussian notch filters versus the normalized filter spacing z_a.

From all the above tests, we conclude that the results are almost identical for properly matched filters. Thus the notion of "matching" NFs to an effectiveness level required by the system appears to be valid as long as the notch ϵ is within the bounds of the perturbation approximation.

4. LUMPED FILTERS

All the above results, both analytical and numerical, have been obtained in the distributed-filtering approximation. As is known, in some cases DM models with lumped filters suffer from specific instabilities. These instabilities can be avoided if the filters are properly placed inside the DM cell.[17] It is therefore necessary to verify that the distributed model adequately approximates a realistic *lumped* configuration with discrete filters.

To this end, we directly simulated the model with lumped Gaussian NFs, varying the spacing z_a between filters in the range $\delta z < z_a < 0.2$, where δz is the numerical resolution in the z dimension. The results are shown in Fig. 7, which demonstrates that the spacing between the filters produces little effect on the final timing jitter. A similar conclusion was obtained by an analytical approach in Ref. 22, justifying the assumption that distributed filtering is an adequate approximation for lumped filtering, provided the filters are close enough.

5. CONCLUSION

In this paper, we have developed a detailed analysis of the dynamics of classical and dispersion-managed solitons guided, in a single frequency-domain channel, by filters of different types, the emphasis being comparison of the results produced by the usual parabolic (etalon) filters and

notch filters. The latter have the form of two finite-width notches with a rectangular or Gaussian shape bounding the transmission channel.

Analytical approximations, based on balance equations for the soliton's energy and momentum, and direct simulations have been used, with the conclusion that the analytical and numerical methods are in a reasonably good agreement, provided that the filters are not too strong, the agreement being especially good for dispersion-managed solitons. We have introduced a concept of filter effectiveness, defined as the strength of the restoring force acting on the soliton in the frequency domain at a fixed value of excess gain. The effectiveness can be optimized by varying the free parameters of a particular type of filter. By use of the free parameters, it is also possible to match a filter to an effectiveness level required by a system without change in the excess gain.

It has been demonstrated that finite-width notch filters are much more efficient than idealized, infinitely narrow ones. Important results are that finite-width notch filters can be as efficient as the etalon (parabolic) filters, and the efficiency is higher for dispersion-managed solitons than for classical ones. Thus it is possible to design a DWDM system without compromising the efficiency of frequency-jitter suppression inside each individual channel.

It was shown that strong notch filters do not give as good a filter effectiveness as is predicted analytically, which is also found for Butterworth filters. Also, DM solitons give numerically higher filter effectiveness than classical solitons, even when the same effectiveness is predicted analytically for both types of solitons.

Besides studying analytically the effectiveness of different types of filters, we have also directly simulated guiding solitons by filters in the presence of random-frequency jitter. We have also demonstrated by direct simulations that the results obtained in the distributed approximation apply as well to a realistic model with lumped filters.

REFERENCES

1. E. A. Golovchenko, A. N. Pilipetskii, and C. R. Menyuk, "Collision-induced timing jitter reduction by periodic dispersion management in soliton wavelength-division-multiplexed transmission," Electron. Lett. **33**, 735–737 (1997).
2. P. V. Mamyshev and L. F. Mollenauer, "Soliton collisions in wavelength-division-multiplexed dispersion-managed systems," Opt. Lett. **24**, 448–450 (1999).
3. A. M. Niculae, W. Forysiak, A. Gloag, J. H. B. Nijhof, and N. J. Doran, "Soliton collisions with wavelength-division-multiplexed systems with strong dispersion management," Opt. Lett. **23**, 1354–1356 (1998).
4. H. Sugahara, H. Kato, and Y. Kodama, "Maximum reductions of collision induced frequency shift in soliton wavelength-division-multiplexed systems with dispersion compensation," Electron. Lett. **33**, 1065–1066 (1997).
5. D. J. Kaup, B. Malomed, and J. Yang, "Interchannel pulse collision in a wavelength-division-multiplexed system with strong dispersion management," Opt. Lett. **23**, 1600–1602 (1998).
6. S. Wabnitz, "Role of the filter spectral profile in the control of soliton transmissions," Opt. Commun. **130**, 89–96 (1996).
7. S. Wabnitz, "Stabilization of sliding-filter soliton wavelength-division-multiplexed transmissions by dispersion compensating fibers," Opt. Lett. **21**, 638–640 (1996).
8. Y. Chen and H. A. Haus, "Collisions in dispersion-managed soliton propagation," Opt. Lett. **24**, 217–219 (1999).
9. L. F. Mollenauer, J. Gordon, and S. Evangelides, "The sliding-frequency guiding filter: an improved form of soliton jitter control," Opt. Lett. **17**, 1575–1577 (1992).
10. M. Hanna, H. Porte, J.-P. Goedgebuer, and W. T. Rhodes, "Soliton optical phase control by use of in-line filters," Opt. Lett. **24**, 732–734 (1999).
11. A. Mecozzi, "Soliton transmission control by Butterworth filters," Opt. Lett. **20**, 1859–1861 (1995).
12. Y. Kodama and A. Hasegawa, "Generation of asymptotically stable optical solitons and suppression of the Gordon–Haus effect," Opt. Lett. **17**, 31–33 (1992).
13. P. V. Mamyshev and L. F. Mollenauer, "Wavelength-division-multiplexing channel energy self-equalization in a soliton transmission line by guiding filters," Opt. Lett. **21**, 1658–1660 (1996).
14. A. Berntson and B. A. Malomed, "Dispersion management with filtering," Opt. Lett. **24**, 507–509 (1999).
15. L. F. Mollenauer, P. V. Mamyshev, and J. P. Gordon, "Effect of guiding filters on the behavior of dispersion-managed solitons," Opt. Lett. **24**, 220–222 (1999).
16. M. Matsumoto, "Analysis of filter control of dispersion-managed soliton transmission," J. Opt. Soc. Am. B **15**, 2831–2837 (1998).
17. M. Matsumoto, "Instability of dispersion-managed solitons in a system with filtering," Opt. Lett. **23**, 1901–1903 (1998).
18. B. Malomed, G. D. Peng, and P. L. Chu, "Soliton wavelength-division multiplexing system with channel-isolating notch filters," Opt. Lett. **24**, 1100–1102 (1999).
19. B. A. Malomed, A. Docherty, P. L. Chu, and G. D. Peng, "Dense wavelength-division-multiplexed soliton systems using channel-isolating notch filters (soliton rail)," in *Massive Wavelength-Division-Multiplexed and Time-Division-Multiplexed soliton transmission systems*, A. Hasegawa, ed. (Kluwer Academic, Boston, 2000); pp. 411–424.
20. S. Orlov, A. Yariv, and S. V. Essen, "Coupled-mode analysis of fiber-optic add-drop filters for dense wavelength division multiplexing," Opt. Lett. **22**, 688–690 (1997).
21. X. J. Gu, "Wavelength-division-multiplexed isolation fiber filter and light source using cascading long-period fiber gratings," Opt. Lett. **23**, 509–511 (1998).
22. M. J. Ablowitz, G. Biondini, S. Chakravarty, and R. Horne, "A comparison between lumped and distributed filter models in wavelength-division multiplexed soliton systems," Opt. Commun. **172**, 211–227 (1999).
23. T. I. Lakoba, J. Yang, D. J. Kaup, and B. A. Malomed, "Conditions for stationary pulse propagation in the strong dispersion management regime," Opt. Commun. **149**, 366–375 (1998).
24. M. J. Ablowitz and G. Biondini, "Multiscale pulse dynamics in communication systems with strong dispersion management," Opt. Lett. **23**, 1668–1670 (1998)
25. T. S. Yang and W. L. Kath, "Analysis of enhanced-power solitons in dispersion-managed optical fibers," Opt. Lett. **22**, 985–987 (1997).
26. V. Zharnitsky, E. Grenier, S. K. Turitsyn, C. Jones, and J. S. Hesthaven, "Ground states of dispersion-managed nonlinear Schrodinger equation," Phys. Rev. E **62**, 7358–7364 (2000).
27. J. H. B. Nijhof, W. Forysiak, and N. J. Doran, "The averaging method for finding exactly periodic dispersion-managed solitons," IEEE J. Sel. Top. Quantum Electron. **6**, 330–336 (2000).
28. K. J. Blow, N. J. Doran, and D. Wood, "Suppression of the soliton self-frequency shift by bandwidth-limited amplification," J. Opt. Soc. Am. B **5**, 1301–1304 (1988).